Paper
Int'l J. of Aeronautical & Space Sci. 17(4), 518–525 (2016)
DOI: http://dx.doi.org/10.5139/IJASS.2016.17.4.518

IJASS
International Journal of Aeronautical and Space Sciences

Effects of High-harmonic Components on the Rayleigh Indices in Multi-mode Thermo-acoustic Combustion Instability

Chang Geun Song*

Department of Safety Engineering, Incheon National University, Incheon 22012, Republic of Korea

Jisu Yoon and Youngbin Yoon***

Department of Mechanical and Aerospace Engineering, Seoul National University, Seoul 08826, Republic of Korea

Young Jin Kim***

Fluid System Engineering Department, KEPCO Engineering and Construction Company, Daejeon 34057 , Republic of Korea

Min Chul Lee****

Department of Safety Engineering, Incheon National University, Incheon 22012, Republic of Korea

Abstract

This paper presents the characteristics of non-fundamental multi-mode combustion instability and the effects of high-harmonic components on the Rayleigh criterion. Phenomenological observations of multi-harmonic-mode dynamic pressure waves regarding the intensity of harmonic components and the source of wave distortion have been explained by introducing examples of second- and third-order harmonics at various amplitudes. The amplitude and order of the harmonic components distorted the wave shapes, including the peak and the amplitude, of the dynamic pressure and heat release, and consequently the temporal Rayleigh index and its integrals.

A cause-and-effect analysis was used to identify the root causes of the phase delay and the amplification of the Rayleigh index. From this analysis, the skewness of the dynamic pressure turned out to be a major source in determining whether multi-mode instability is driving or damping, as well as in optimizing the combustor design, such as the mixing length and the combustor length, to avoid unstable regions. The results can be used to minimize errors in predicting combustion instability in cases of high multi-mode combustion instability. In the future, the amount of research and the number of applications will increase because new fuels, such as fast-burning syngases, are prone to generating multi-mode instabilities.

Key words: gas turbine combustor, combustion instability, high multi-mode instability, Rayleigh index calculation

1. Introduction

Lean premixed, pre-vaporized combustion technology has been utilized for low-NO_x emission and high combustion efficiency in propulsion engines and industrial gas turbines. Unfortunately, this low-NO_x characteristic necessitates a trade-off with the thermos-acoustic combustion instabilities that often cause fatal accidents. Thus, several studies have been conducted to understand and alleviate combustion instabilities. Previous research contributed greatly to the understanding of combustion instability mechanisms, such as flame-vortex interaction [1, 2], feedback on fluctuations in acoustic pressure, mixture velocity, equivalence and heat release [3, 4], perturbation of entropy [5, 6], processing

* Professor
** Ph. D Student
*** Ph. D
**** Professor, Corresponding author: LMC@inu.ac.kr

Received: September 14, 2015 Revised: October 4, 2016 Accepted: October 20, 2016

http://ijass.org pISSN: 2093-274x eISSN: 2093-2480

vortex core (PVC) [7, 8], interference between acoustic and convective disturbances [9], and the temporal fluctuation in swirl strength [10-12]. However, it is almost impossible to derive a universal mechanism for interpreting and predicting complex nonlinear combustion instability phenomena [13, 14] because the governing mechanisms differ in combustor geometry, fuel specification, and air-supplying conditions. Moreover, most studies considered combustion instability in a single mode of natural fundamental frequency but not in a real engine. In practical systems, combustion instability can have two or more harmonic or non-harmonic modes; thus, the pressure wave could be distorted because of the superposition of these multi-modes. This distortion can cause significant errors in understanding and predicting combustion instability. Lee et al. [15] investigated the causes of this multi-mode combustion instability in specific compositions of $H_2/CO/CH_4$ syngases. These phenomena were previously reported in the self-excited combustion instability of multi-modes [16] or in the transition from a fundamental mode to its higher harmonic mode [17-19]. In the present paper, a time lag analysis, which is an important analytical method used to understand and predict instability driving and damping, is developed for multi-mode instability. Using the derivation of characteristic time scales, the errors caused by treating the multi-mode as a single mode are reduced, and a quantitative index for assuming the multi-mode as a single mode is suggested. In addition, case studies of various harmonic-amplitude pressure waves are conducted to enhance the comprehension of practical multi-mode situations.

2. Phenomenological description of multi-mode combustion instability

Multi-mode instability can be classified into two kinds: non-harmonic instability and harmonic instability. In non-harmonic instability, the longitudinal mode with a high-frequency radial, transverse, or circumferential mode often generates non-harmonic multi-mode instability. In particular, rocket combustors with a short length and a large radius are prone to generating high-frequency mode instability, the so-called screeching mode, but gas turbine combustors seldom generate any mode but the longitudinal. Because the amplitude of screeching instability is small, it can usually be considered negligible or approximated as a single mode. The source of non-harmonic instability includes noise that should be filtered when measuring the signal. Thus, this study focuses on harmonic instability and not on non-harmonic instability.

In harmonic instability, only one mode among the longitudinal, radial, and circumferential modes dominates the instability phenomena; therefore, only the fundamental mode and its harmonics appear in pressure waves. Fig. 1(a) illustrates standing-wave examples of the first longitudinal mode and its second- and third-order harmonics when the combustion chamber is assumed to be a closed-inlet and closed-outlet cylindrical cavity. The amplitude of the dynamic pressure is always zero at each node, and the number of nodes in each mode is equal to the mode order. Although the first mode is usually dominant, the second mode or higher can also be significant in some cases, especially in the combustion of fast-burning gases [15]. Fig. 2 shows an example of a pressure wave in multi-mode combustion instability measured in a General Electric 7EA gas turbine firing $H_2/CO/CH_4$ syngas. Wave (A), at a frequency of 1020 Hz, is distorted, and Wave (B), at a frequency of 762 Hz, is undistorted. The reason for the distortion is shown in Fig. 3, with the frequency domain plot of the pressure waves in Fig. 2. Wave (A) is distorted because of the large amplitude of the harmonic components, whereas Wave (B) is undistorted because of the small amplitude of the harmonic components.

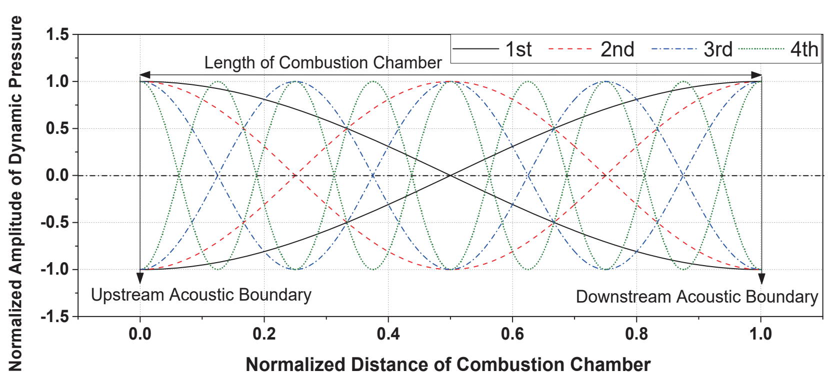

Fig. 1. Normalized pressure wave configurations in the first, second, and third longitudinal modes. The normalized distance of the combustion chamber is 0.0 at the damping plane and 1.0 at the combustor exit.

This distortion can be affected by the harmonic order, as well as the relative amplitudes of the harmonic components.

3. Wave distortion from multi-mode combustion instability

To understand the wave distortion in detail, case studies were conducted on representative second- and third-order harmonic combinations as shown in Table 1. Fig. 4 shows the various shapes of the pressure waves that correspond to the representative combinations of the first, second, and third modes. The wave equation used in Fig. 4 is as follows:

$$f(t) = A\sin(wt) + B\sin(2wt) + C\sin(3wt) \quad (1)$$

where A, B, and C are the amplitudes of the first, second, and third pressure waves, and w is the period of the first mode. To offer a simpler description, w is assumed to be 2π/1000, and the amplitude ratios are defined in the following equations:

$$AR_{p2\text{-}1} = \frac{B}{A} \quad (2)$$

$$AR_{p3\text{-}1} = \frac{C}{A} \quad (3)$$

As shown in Fig. 4(a), the peak of the pressure wave moves to the left, and the wave distortion increases as $AR_{p2\text{-}1}$ increases. This could be attributed to the fact that the larger harmonic component distorts the temporal variation in the pressure wave and shifts the upper and low peaks to the left and right, respectively. The inversion from positive to negative does not appear in cases 1, 2, and 3, but it does appear in case 4. The criterion for the existence of this inversion is $AR_{p2\text{-}1}$ because the wave in case 3 is tangential to

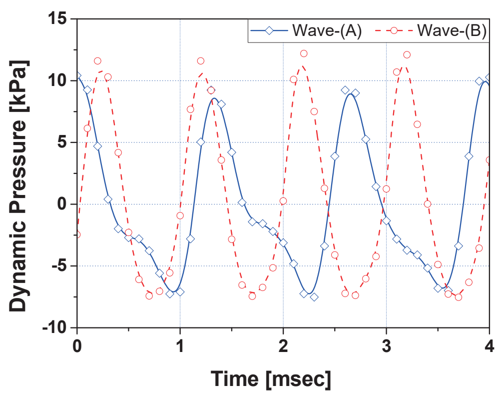

Fig. 2. Example of pressure waves in multi-mode combustion instability measured in a GE7EA gas turbine firing $H_2/CO/CH_4$ syngas. Wave (A) is distorted, and Wave (B) is undistorted.

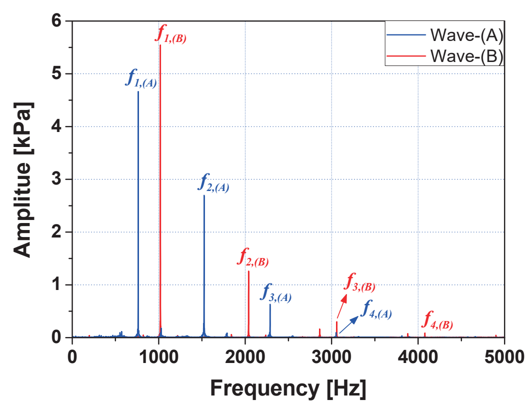

Fig. 3. Frequency domain plot of the pressure waves shown in Fig. 2.

Table 1. Case study conditions and standing wave equations for representative second- and third-order harmonics.

Case Number	$AR_{p2\text{-}1}$	$AR_{p3\text{-}1}$	Wave Equation
Ref	0	0	$f(t) = 1\sin(wt)$
1	0.25	0	$f(t) = 0.8\sin(wt) + 0.2\sin(2wt)$
2	0.5	0	$f(t) = (2/3)\sin(wt) + (1/3)\sin(2wt)$
3	1	0	$f(t) = 0.5\sin(wt) + 0.5\sin(2wt)$
4	0.25	0.25	$f(t) = 0.8\sin(wt) + 0.2\sin(2wt) + 0.2\sin(3wt)$
5	0.25	0.5	$f(t) = 0.8\sin(wt) + 0.2\sin(2wt) + 0.4\sin(3wt)$
6	0.5	0.25	$f(t) = (2/3)\sin(wt) + (1/3)\sin(2wt) + (1/6)\sin(3wt)$
7	0.5	0.5	$f(t) = (2/3)\sin(wt) + (1/3)\sin(2wt) + (1/3)\sin(3wt)$
8	2	1	$f(t) = (1)\sin(wt) + (2)\sin(2wt) + (1)\sin(3wt)$

the x-axis at t = π msec.

Similarly, the third harmonic multi-mode shown in Fig. 4(b) follows this distortion trend. The pressure peak moves to the left, and the wave becomes increasingly distorted, forming three peaks at $AR_{p3\text{-}1} > 0.5$ as $AR_{p3\text{-}1}$ increases because the additional superposition of the third-order harmonic component becomes increasingly distorted and the positive peak is skewed. In this study, skewness means the peak shift from the original wave without harmonics to the left (or right), and distortion means the difference in shape from the original wave without harmonics to the changed wave. As $AR_{p3\text{-}1}$ increases, the three peaks corresponding to the third-order harmonics appear clearly. However, the third peak cannot overcome the first mode trend in cases 4, 5, 6, and 7 ($AR_{p2\text{-}1}$ and $AR_{p3\text{-}1} < 1$). The general trend of the first mode does not change because the largest amplitude is the first-order harmonic, and the harmonic mode with the largest amplitude governs the overall trend.

The wavier dynamic pressure indicates sensitive alternation in the instability indices, such as the Rayleigh index, with respect to time. Thus, the measurement and calculation of these indices and the synchronization of p' with q' should be more accurate in multi-mode instability than in single mode instability; otherwise, errors proportional to the harmonic intensity could result. Additionally, the wave distortion and transition to higher harmonics significantly affect the accuracy of the predicting methods, the Rayleigh index, and the time lag analysis. Therefore, a detailed investigation of the Rayleigh index of multi-mode harmonic instability is conducted in the following sections.

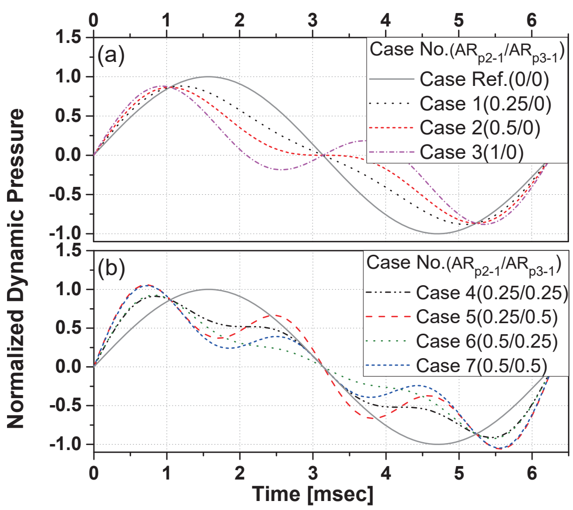

Fig. 4. Representative wave shapes of the combinations of first-, second-, and third-order harmonics. (a) Fundamental mode with only second-order harmonics ($AR_{p3\text{-}1}$= 0) (b) Fundamental mode with second- and third-order harmonics.

4. Effects of harmonic components on the Rayleigh index

4.1. Rayleigh criterion

Most mechanisms of thermo-acoustic combustion instability are based on the Rayleigh criterion:

$$IRI = \int_V\int_T p'(x,t)q'(x,t)dtdv = \int_V\int_T RI(x,t)dtdv \geq \int_V\int_T\sum_i L_i(x,t)dtdv \quad (4)$$

where *IRI*, *p*', *q*', *RI*, and L_i, are integrals in the Rayleigh index, instantaneous pressure fluctuation, instantaneous heat release rate, Rayleigh index, and i-th damping coefficient, respectively. This criterion indicates that p' and q' should be in phase to drive the instabilities and out-of-phase to dampen the instabilities [20]. In the Rayleigh criterion, the linear superposition of harmonic waves is established for neither the pressure wave nor the heat because the distorted pressure propagates upstream to the fuel injector and plugs the fuel flow rate, causing fluctuation in the equivalence ratio, consequently generating a heat-release rate fluctuation at the flame. Nothing changes except the shapes of the pressure wave and the distorted wave itself, which should be considered in the calculation of the RI for the multi-mode. However, the multi-mode RI should be cautiously calculated because a distorted p' couples with an undistorted q'. The continuous existence of the flame and the burning of the entrapped unburned gas at any recirculation zone of the combustor restores the distortion of p' to be sinusoidal in q'. Therefore, consideration of the distorted p' with an undistorted q' to obtain the time series RI decreases error in the prediction of instability in driving and damping.

4.2. Time series Rayleigh index for second-order harmonics

The one-dimensional longitudinal mode is the simplest and the most representative mode in combustion instability. Thus, this mode with second harmonics was selected in the first investigation of multi-mode instability. As shown in Fig. 5, the time series RI was obtained for various $AR_{p2\text{-}1}$ in changing the phase angle between p' and q' ($\theta_{p'\text{-}q'}$) from 0° to 315°. First, as anticipated, the maximum RI for a single mode ($AR_{p2\text{-}1} = 0$) appeared when p' was exactly collapsed with q' ($\theta_{p'\text{-}q'} = 0°$), while the minimum was at $\theta_{p'\text{-}q'} = 180°$. When $\theta_{p'\text{-}q'}$ was 90° or 270° (within the maximum and the minimum), the integral of the RI for periodic time was zero.

These results satisfied the Rayleigh criterion well in which p' and q' should be in phase to drive the instabilities and out-of-phase to dampen the instabilities. As shown in Fig. 5(a), the RI has two peaks in a cycle, which means the frequency is doubled in driving and damping because the positive p' couples with the positive q' and the negative p' couples with the negative q'. Otherwise, in the middle of driving and damping ($\theta_{p'\text{-}q'} = 90°$ or $270°$) in the case of $AR_{p2\text{-}1} = 0.75$ and 1, a skewed and small peak was observed, and the frequency was not doubled. A similar phenomenon of frequency doubling and non-doubling was reported in a recent investigation of multi-mode combustion instability in which the integrated Rayleigh index (IRI) of a two-dimensional third and fourth harmonic longitudinal multi-mode was observed [15]. As the $AR_{p2\text{-}1}$ continuously increased, the RI became more skewed, finally followed by the second-mode behavior of $AR_{p2\text{-}1} > 1$. It is also notable that the RI had a negative value even in the exact in-phase ($\theta_{p'\text{-}q'} = 0°$) when $AR_{p2\text{-}1}$ was above 0.5. This inversion was attributed to the effect of intense harmonic components, and the region of inversion was larger the $AR_{p2\text{-}1}$ was increased. Based on the results of the one-dimensional second harmonic multi-mode analysis, it can be concluded that the temporal variation in the RI was significantly affected by $\theta_{p'\text{-}q'}$ as well as by $AR_{p2\text{-}1}$. Therefore, additional consideration of the multi-mode differentiated from the single mode is necessary when the IRI is obtained or the Rayleigh criterion is applied and the analysis derived from it.

4.3. Integrated Rayleigh index for second-order harmonic components

The integral of the RI can be used for the criterion of the instability acceleration and deceleration. If IRI > 0, then the combustion system becomes unstable; otherwise, vice versa. To understand the effect of harmonic intensity on the overall generation and decaying of instability, the IRI of various amplitude ratios of harmonic components was investigated. As illustrated in Fig. 6, the IRI is sinusoidal although the pressure wave is distorted because the IRI is not related to

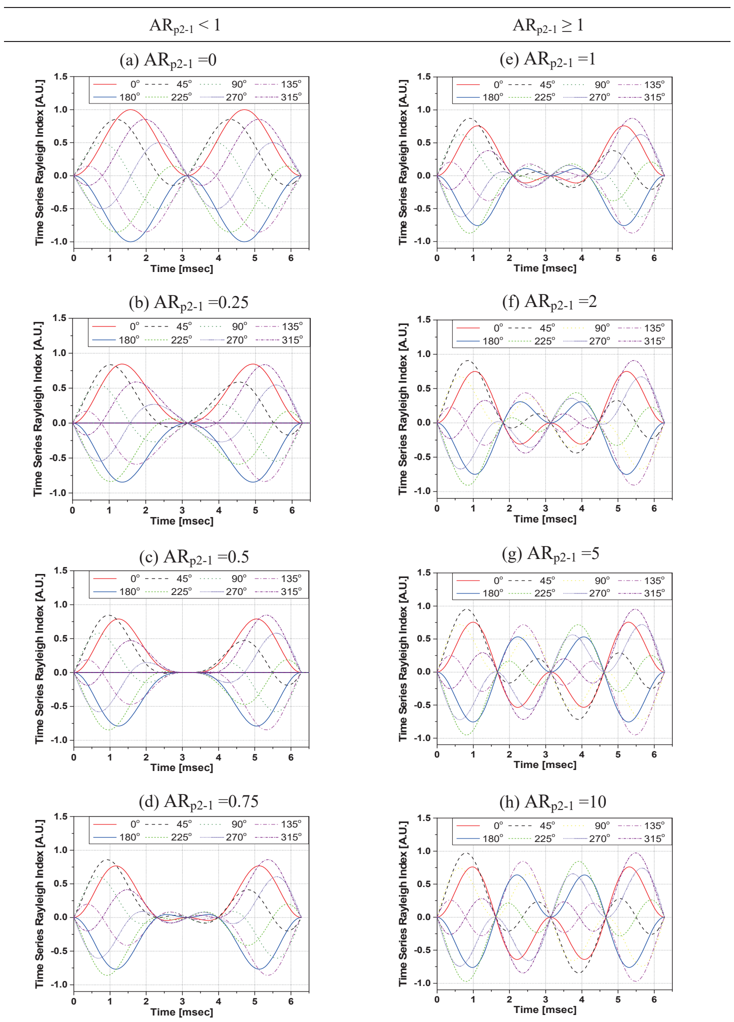

Fig. 5. Comparison of the wave shapes of the time series Rayleigh indices with respect to $AR_{p2\text{-}1}$.

DOI: http://dx.doi.org/10.5139/IJASS.2016.17.4.518

the pressure wave itself but to the coupling of p' and q' with respect to $\theta_{p'-q'}$. Maximum instability can be generated at $\theta_{p'-q'} = 0$ without higher harmonics. The pressure wave distortion caused by the harmonic components shifts the maximum IRI from zero to over zero. Similarly, the minimum IRI also moves from left to right as the AR_{p2-1} is increased. The instability driving/damping criterion at which IRI = 0 moves the same amount and in the same direction as the maximum and minimum of the IRI. These results indicate that instability can be wrongly determined unless the exact waveform has not been considered for large amounts of harmonic multi-mode. This mistake can be amended by full consideration of the wave shape, including distortions and the introduction of additional terms, such as skewness time [15] in time lag analysis.

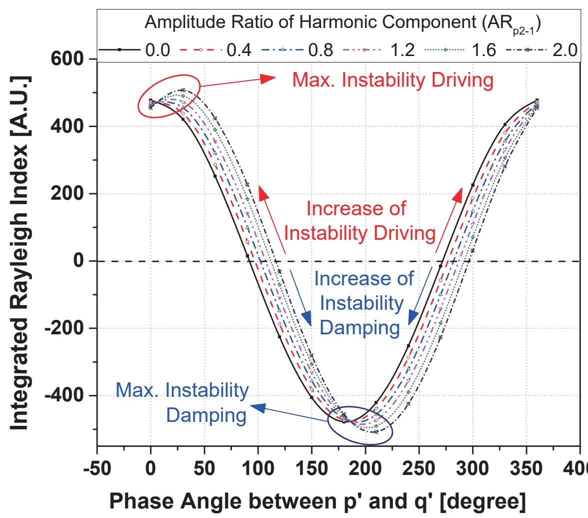

Fig. 6. Integrated Rayleigh indices for various amplitude ratios of second-order harmonic components.

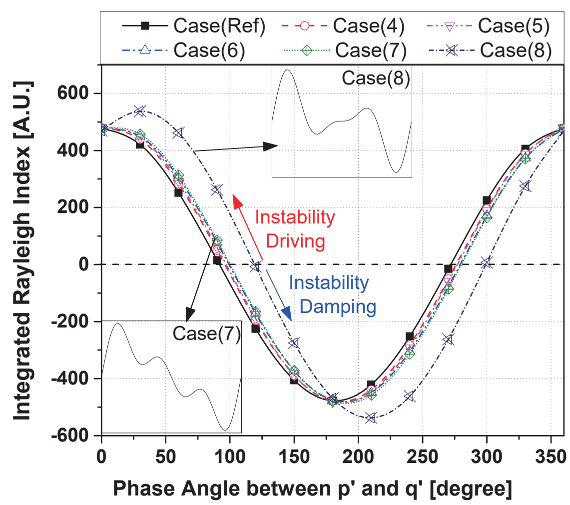

Fig. 7. Integrated Rayleigh indices in various cases of second- and third-order multi-mode instability.

4.4. Integrated Rayleigh index for second- and third-order harmonic components

Cases 4, 5, 6, 7, and 8, which are shown in Table 1, were selected to understand the effect of third-order multi-mode harmonics on the characteristics of instability.

In Fig. 7, the IRI in the second- and third-order harmonic components show trends similar to those in the second-order harmonic components. The sinusoidal IRI moves right as the AR_{p2-1} increases, and AR_{p3-1} and the amplitude of the IRI are almost proportional to the increment in the total harmonic amplitude. In case 8, the large second- and third-order harmonic amplitudes highly skewed ’ , which resulted in the phase delay and magnification of the IRI. This skewness effect could be attributed to the amplitude of the high harmonic components rather than the higher order of harmonics. In contrast, in case 7, p' is highly distorted rather than skewed, so neither phase delay nor magnification is noticeable compared to case 8.

4.5. Root cause analysis of the temporal RI and the IRI

To better understand the detailed relationship between the harmonics and the RI or the IRI and to investigate the root cause of the variation in the temporal RI and the IRI, the cause-and-effect diagram in Fig. 8 summarizes the results. In this diagram, skewness means the peak shift from the original wave without harmonics to the left (or right), and distortion means the difference in shape from the original wave without harmonics to the changed wave. Multi-mode combustion instability might have various orders and amplitudes of the harmonic components. The change in order does not alter the distortion or the skewness as much as it does the change

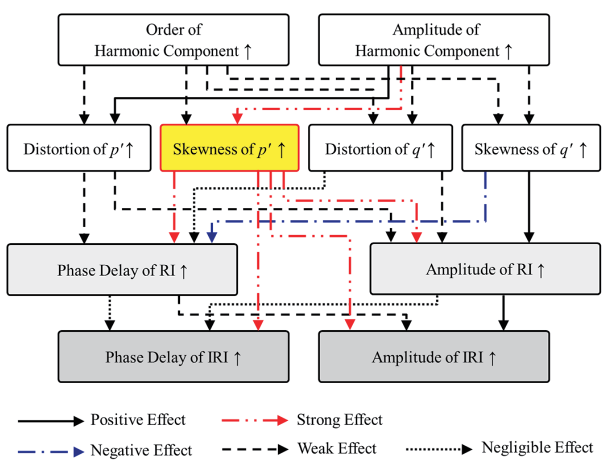

Fig. 8. Cause-and-effect diagram of the relationship between the order and the amplitude of the harmonic component and the Rayleigh index and the integrated Rayleigh index.

in amplitude. The q' is not the root element in the cause-and-effect analysis because it is not affected by the changes in harmonics as much as p' is changed. The phase delay and the amplitude of the temporal IR and IRI are mainly affected by the skewness of ', which is caused by the change in the amplitude of the harmonic component. The highlighted "red" tree is the backbone in the mechanism of multi-mode combustion instability.

5. Conclusion

The characteristics of non-fundamental multi-mode combustion instability and the effects of the high-harmonic components on the Rayleigh criterion were investigated with phenomenological observations and the analysis of the RI and the IRI. Based on the results of the analysis, the following conclusions were derived:

(1) The high harmonic superposition phenomenon has long been ignored because it rarely occurs in a gas turbine combustor. However, non-ignorable multi-mode behavior was investigated by adapting fast-burning high hydrogen fuels. A particular characteristic of the multi-mode is the point movement of driving/damping inversion because the stable region can be wrongly determined as unstable and vice versa.

(2) The harmonic component alters the shapes of p' and q', and the peak shift (skewness) and the amplitude change in p' are the root causes of the phase delay and magnification of the RI and the IRI. Fig. 8 summarizes the relationship between the elements of multi-mode instability. The application and analysis should be cautiously conducted because of unexpected particular behaviors; for example, the phase delay in the IRI is not directly affected by the RI.

(3) The importance of wave shape distortion and skewness was clarified in determining whether instability occurred in driving or damping. When the multi-mode analysis method is applied to the single mode, three amendments should be considered: 1) reflection of pressure wave distortion; 2) regeneration of the RI map from the q' if possible; and 3) recalculation of the temporal variation of RI from the distorted ' and the less distorted q' by integrating RI cubes or maps in the volume or area.

(4) When designing a combustor for a gas turbine or propulsion engine, the optimal selection of combustor geometry, such as the mixing length and the combustor length, which can avoid unstable regions, is important in order to attenuate the likelihood of failure caused by high multi-mode combustion instability. Therefore, caution is necessary from the design stage to the verification test.

(5) Because there is no model of universal combustion instability, the prediction and analysis of combustion instability should be cautiously implemented on a case-by-case basis. The present study attempted to minimize errors in the prediction of combustion instability. The results presented here could contribute to future research and applications of high multi-mode combustion instability.

Acknowledgement

This work was supported by the Incheon National University Research Grant in 2015.

References

[1] Külsheimer, C. and Buchner, H., "Combustion Dynamics of Turbulent Swirling Flames", *Combustion and Flame*, Vol. 131, 2002, pp. 70–84.

[2] Schadow, K. C., Gutmark, E., Parr, T. P., Parr, D. M., Wilson, K. J. and Crump, J. E., "Large-Scale Coherent Structures as Drivers of Combustion Instability", *Combustion Science and Technology*, Vol.64, 1989, pp. 167–186.

[3] Lieuwen, T., Torres, H., Johnson, C. and Zinn, B. T., "A Mechanism of Combustion Instability in Lean Premixed Gas Turbine Combustors", *Journal of Engineering for Gas Turbine and Power*, Vol. 123, 2001, pp. 182–189.

[4] Seo, S., "Combustion Instability Mechanism of a Lean Premixed Gas Turbine Combustor", *Journal of Mechanical Science and Technology*, Vol. 176, 2003, pp. 906–913.

[5] Sattelmayer, T., "Influence of the Combustor Aerodynamics on Combustion Instabilities from Equivalence Ratio Fluctuations", *Journal of Engineering for Gas Turbine and Power*, Vol. 123, 2003, pp. 11–19.

[6] Eckstein, J., Freitag, E., Hirsch, C. and Sattelmayer, T., "Experimental Study on the Role of Entropy Waves in Low-Frequency Oscillations in a RQL Combustor", *Journal of Engineering for Gas Turbine and Power*, Vol. 128, 2006, pp. 264–270.

[7] Steinberg, A. M., Boxx, I., Stohr, M., Carter, C. D. and Meier, W., "Flow-Flame Interactions Causing Acoustically Coupled Heat Release Fluctuations in a Thermo-Acoustically Unstable Gas Turbine Model Combustor", *Combustion and Flame*, Vol. 157, 2010, pp. 2250–2266.

[8] Syred, N., "A Review of Oscillation Mechanisms

and the Role of the Precessing Vortex Core (PVC) in Swirl Combustion Systems", *Progress in Energy and Combustion Science*, Vol. 32, 2006, pp. 93–161.

[9] Kim, K. T. and Santavicca, D. A., "Interference Mechanism of Acoustic/Convective Disturbances in a Swirl-Stabilized Lean-Premixed Combustor", *Combustion and Flame*, Vol. 160, 2013, pp. 1441-1457.

[10] Komarek, T. and Polifke, W., "Impact of Swirl Fluctuations on the Flame Response of a Perfectly Premixed Swirl Burner", *Journal of Engineering for Gas Turbine and Power*, Vol. 132, 2010, 061503.

[11] Wang, S. and Yang, V., "Unsteady Flow Evolution in Swirl Injectors with Radial Entry. Ⅱ. External Excitations", *Physics of Fluids*, Vol. 17, 2005, 045107.

[12] Acharya, V., Shin, D. H. and Lieuwen, T., "Swirl Effects on Harmonically Excited, Premixed Flame Kinematics", *Combustion and Flame*, Vol. 159, 2012, pp. 1139–1150.

[13] Syred, N., "A Review of Oscillation Mechanisms and the Role of the Precessing Vortex Core (PVC) in Swirl Combustion Systems", *Progress in Energy and Combustion Science*, Vol. 32, 2006, pp. 93–161.

[14] Tran, N., Ducruix, S. and Schuller, T., "Damping Combustion Instabilities with Perforates at the Premixer Inlet of a Swirled Burner", *Proceedings of Combustion Institut*e, Vol. 32, 2009, pp. 2917-2924.

[15] Lee, M. C., Yoon, J., Joo, S., Kim, J., Hwang, J. and Yoon, J., "Investigation into the Cause of High Multi-Mode Combustion Instability of H_2/CO/CH_4 Syngas in a Partially Premixed Gas Turbine Model Combustor", *Proceedings of Combustion Institute*, Vol. 35, 2015, pp. 3263-3271.

[16] Sterling, J. D. and Zukoski, E. E., "Nonlinear Dynamics of Laboratory Combustor Pressure Oscillations", *Combustion Science and Technology*, Vol. 77, 1991, pp. 225–238.

[17] Billoud, G., Galland, M. A., Huu, C. H. and Candel, S., "Adaptive Active Control of Combustion Instabilities", *Combustion Science and Technology*, Vol. 81, 1992, pp. 257–283.

[18] Gulati, A. and Mani, R., "Active Control of Unsteady Combustion-induced Oscillations", *Journal of Propulsion and Power*, Vol.8, 1992, pp. 1109–1115.

[19] Fleifil, M., Hathout, M. P., Annaswamy, A. M. and Ghoniem, A. F., "The Origin of Secondary Peaks with Active Control of Thermoacoustic Instability", *Combustion Science and Technology*, Vol. 133, 1998, pp. 227-265.

[20] Rayleigh, L., *The Theory of Sound*, Dover, NY, 1945.